Identification of *Rhodococcus fascians* cytokinins and their modus operandi to reshape the plant

Ine Pertry[a,b,1], Kateřina Václavíková[c,d,1], Stephen Depuydt[a,b,1], Petr Galuszka[d], Lukáš Spíchal[c], Wim Temmerman[b], Elisabeth Stes[a,b], Thomas Schmülling[e], Tatsuo Kakimoto[f], Marc C. E. Van Montagu[a,b,2], Miroslav Strnad[c], Marcelle Holsters[a,b], Petr Tarkowski[c,d,2], and Danny Vereecke[a,b,2]

[a]Department of Plant Systems Biology, Flanders Institute for Biotechnology, Technologiepark 927, 9052 Gent, Belgium; [b]Department of Molecular Genetics, Ghent University, 9052 Gent, Belgium; [c]Laboratory of Growth Regulators, Palacký University and Institute of Experimental Botany ASCR, Šlechtitelů 11, 783 71 Olomouc, Czech Republic; [d]Department of Biochemistry, Faculty of Science, Palacký University, 783 71 Olomouc, Czech Republic; [e]Institut für Biologie/Angewandte Genetik, Freie Universität Berlin, Albrecht-Thaer-Weg 6, 14195 Berlin, Germany; and [f]Department of Biological Sciences, Graduate School of Science, Osaka University, Toyonaka, Osaka 560-0043, Japan

Decades ago, the importance of cytokinins (CKs) during *Rhodococcus fascians* pathology had been acknowledged, and an isopentenyltransferase gene had been characterized in the *fas* operon of the linear virulence plasmid, but hitherto, no specific CK(s) could be associated with virulence. We show that the CK receptors AHK3 and AHK4 of *Arabidopsis thaliana* are essential for symptom development, and that the CK perception machinery is induced upon infection, underlining its central role in the symptomatology. Three classical CKs [isopentenyladenine, *trans*-zeatin, and *cis*-zeatin (cZ)] and their 2-methylthio (2MeS)-derivatives were identified by CK profiling of both the pathogenic *R. fascians* strain D188 and its nonpathogenic derivative D188–5. However, the much higher CK levels in strain D188 suggest that the linear plasmid is responsible for the virulence-associated production. All *R. fascians* CKs were recognized by AHK3 and AHK4, and, although they individually provoked typical CK responses in several bioassays, the mixture of bacterial CKs exhibited clear synergistic effects. The *cis*- and 2MeS-derivatives were poor substrates of the apoplastic CK oxidase/dehydrogenase enzymes and the latter were not cytotoxic at high concentrations. Consequently, the accumulating 2MeScZ (and cZ) in infected *Arabidopsis* tissue contribute to the continuous stimulation of tissue proliferation. Based on these results, we postulate that the *R. fascians* pathology is based on the local and persistent secretion of an array of CKs.

phytopathogen | actinomycete | phytohormone

The fine-tuned balance of plant regulators has a key role in the growth and development of plants. Many plant-associated bacteria can influence their hosts by either modulating the phytohormone production or producing the phytohormones themselves. The main advantages for the bacteria are increased nutrient release, suppression of defense, and/or disease establishment (1, 2). Hyperplasia-inducing bacteria, such as *Pantoea agglomerans* and *Pseudomonas savastanoi*, secrete high amounts of cytokinins (CKs) and auxins to facilitate or initiate gall development (3, 4), and *Agrobacterium tumefaciens* genetically transforms plant cells to convert them into CK and auxin (and opine) factories (5).

In contrast to the undifferentiated galls induced by the bacteria mentioned above, the Actinomycete *Rhodococcus fascians* that shares persistence strategies with the closely related human pathogen *Mycobacterium tuberculosis* (6) provokes the formation of differentiated leafy galls, consisting of numerous shoot primordia whose further outgrowth is inhibited (7). The shooty symptoms can be partially mimicked by exogenous addition of CKs (8, 9), and analyses of culture supernatants of different nonisogenic virulent and avirulent *R. fascians* strains grown under rich culture conditions identified 11 different CKs: methylaminopurine, 2-methylthio-isopentenyladenine (2MeSiP), iP, *cis*-zeatin (cZ), *trans*-zeatin (tZ), dihydrozeatin (DZ), 2MeScZ, and their respective ribosides (10–14). Except for iP, the primary source for these CKs was assumed to be tRNA (13). However, contradictory results made it impossible to correlate the amount of secreted CKs, the virulence of the

producing strain, and their presence in infected plants (7, 9, 13–18). Also, the levels of some CKs detected in cultures of *A. tumefaciens* and *P. savastanoi* were up to 1,000-fold higher than those of virulent *R. fascians* strains (14, 19). Then, why is only *R. fascians* able to induce shoots at the infection site?

The role of CKs in *R. fascians*-induced symptoms was strongly supported by the identification of an isopentenyltransferase (*ipt*) gene on a linear virulence plasmid (15) and its strict correlation with virulence (20). Also, *Streptomyces turgidiscabies*, the only other bacterial species known to induce differentiated leafy galls, differs from other scab-causing Streptomycetes by the unique acquisition of a *R. fascians*-like *ipt* gene (21). The *ipt* gene of *R. fascians* strain D188 was expressed only under very specific conditions that might reflect the presence of the host and, importantly, differ from those used in the past to identify and quantify the bacterial CKs (15, 22).

Here, we studied the role of the bacterial CKs in the *R. fascians* pathology by assessing the involvement of the CK perception machinery of *Arabidopsis thaliana* in symptom development. The CK profile of 2 near-isogenic *R. fascians* strains, differing only in the presence of the linear plasmid, was reassessed, and the biological activity of the identified CKs, their *in planta* stability, and their capacity to activate the CK signaling cascade in *Arabidopsis* was determined. Based on the results, we postulate a model on the mode of action of the bacterial CKs during symptomatology.

Results

The *Arabidopsis* CK Receptors AHK3 or AHK4 Are Required for Symptom Development. The stunted and bushy phenotype that develops in *Arabidopsis* upon *R. fascians* infection is correlated with a strong CK response, including the activation of homeostatic mechanisms and expression of A-type response regulators (9). To assess their role in disease, several CK receptor mutants (23, 24) were infected and their response evaluated over time. Single receptor mutants in *ahk2*, *ahk3*, and *ahk4*, and the double mutants *ahk2ahk4* and *ahk2ahk3* developed regular *R. fascians* disease symptoms [see supporting information (SI) Fig. S1]. In contrast, the *ahk3ahk4* mutant, in which AHK2 is the only functional CK receptor, and the triple knockout mutant did not respond to the pathogen (Fig. 1), demonstrating that AHK3 or AHK4, but not AHK2, are necessary for symptom development.
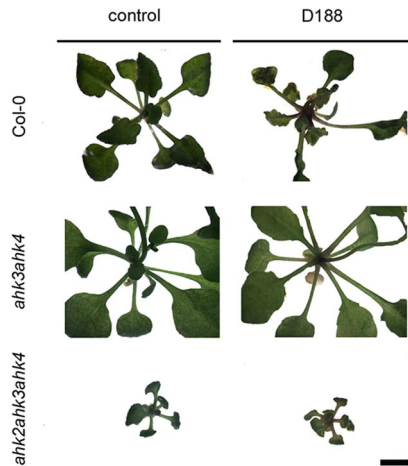
PLANT BIOLOGY

Fig. 1. Response of double and triple CK receptor mutants upon mock inoculation or infection with *R. fascians* D188 at 17 dpi. Responsiveness is evidenced by activated axillary meristems and serrated leaf margins. All images were taken at the same magnification. (Scale bar, 1 cm.)

We evaluated the spatiotemporal dynamics of the CK perception machinery by means of histochemical analysis of infected *AHK3:GUS* and *AHK4:GUS* lines (24). The *AHK3* promoter activity was very high in the shoot of mock-inoculated controls and in symptomatic tissues (Fig. S2). The *AHK4* expression was activated from 4 days post infection (dpi) onward both in the preformed leaves and in induced symptomatic tissues, indicating broadening of the expression domain. The induction level was stronger in the youngest leaves (Fig. 2), which may be correlated with the colonization degree. Together, these data prove the crucial role of the bacterial CKs in the pathology.

***R. fascians* Produces a Spectrum of CKs That Are Recognized by AHK3 and AHK4.** To identify the bacterial CKs responsible for virulence, the CK profiles were determined of the pathogenic strain D188 and its nonpathogenic plasmid-free derivative D188–5, grown overnight in minimal medium under control and optimized conditions for virulence gene expression (22). The levels of O- and 9-glucoside derivatives, benzylaminopurine, *p*-, *m*-, and *o*-topolin, and DZ were below detection limit, and the CK ribosides had the same profile as their bases, but were produced at concentrations <1 nM (data not shown). Interestingly, both strains produced the same spectrum of CK bases (Fig. 3), implying that the *R. fascians* D188 virulence is related to CK threshold levels rather than to specialized molecules. Indeed, although the 2MeSiP levels were independent of the linear plasmid, the 2MeScZ (2-fold), iP (5-fold), and cZ (2-fold) levels were significantly higher for D188 than for D188–5. The concentration of tZ was 100-fold lower than that of the other CKs, but a 2-fold increase was observed in the presence of the linear plasmid (Fig. 3). 2MeStZ was detected in D188 supernatants only, but the levels were very close to the detection limit (data not shown). However, the CK levels did not differ between noninducing or
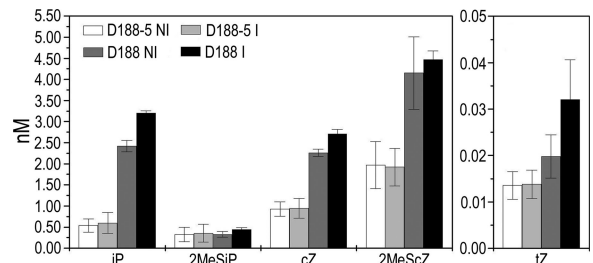

Fig. 3. Cytokinin profile of the supernatant of near-isogenic *R. fascians* strains D188 and D188–5 grown under noninducing (NI) and inducing (I) conditions for virulence gene expression. Error bars represent SDs (*n* = 3).

inducing conditions for virulence gene expression, suggesting that in vitro growth conditions are not adequate to support efficient CK production.

These data show that 2MeScZ is the most abundant CK produced by strain D188, followed by iP and cZ. These CK levels are correlated with the presence of the virulence plasmid and, hence, probably with symptom development. In the literature, little biological activity is attributed to cZ and 2MeScZ (25); therefore, the ability of AHK3 and AHK4 to recognize the 6 CK bases produced by *R. fascians* was tested in an *Escherichia coli*-based receptor-binding assay (26). The dose–response curves show that the 2MeS-derivatives bind to both CK receptors, although less efficiently than the classical CKs (Fig. S3).

Accumulation of Specific *R. fascians* CKs *in Planta* Results from Inadequate Homeostasis. If the CKs identified above were biologically important during *R. fascians* infection, they would be expected to be stable *in planta* and to occur in infected tissues. Previous studies have demonstrated that upon infection with *R. fascians* the overall CK content decreased due to rapidly activated CK homeostatic mechanisms (9, 14, 18). Because 2MeS-type CKs had never been considered, we analyzed the CK content of infected *Arabidopsis* shoot material before visible symptoms (2 dpi), at the onset of tissue deformation (7 dpi), and after fully established disease (35 dpi). Except for tZ, the CK bases were initially more abundant in infected tissues than in mock-inoculated controls (Fig. 4). Bacterial virulence gene expression *in planta* starts at 2 dpi (I.P., unpublished results; see ref. 27), and the CK biosynthetic machinery of the plant is repressed early upon infection (9); therefore, the CK accumulation can be attributed directly to the bacteria. Over time, iP, tZ, 2MeSiP, and 2MeStZ levels decreased, but 2MeScZ and, especially, cZ accumulated (Fig. 4). Similar patterns were observed for the CK ribosides (data not shown).

The build-up of cZ and 2MeScZ might result from the inability of CK oxidase/dehydrogenases (CKXs) to degrade these CKs. Because *R. fascians* resides in the apoplast during its endophytic life phase (28, 29), the apoplastic enzymes CKX2, CKX4, and CKX6 of *Arabidopsis* (30) are probably important for the CK homeostasis during the *R. fascians* pathology. Partially purified recombinant CKX2, CKX4, and CKX6 proteins were used in in vitro assays with
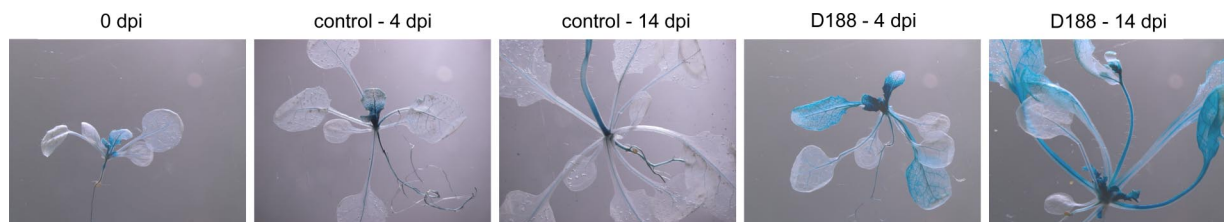

Fig. 2. Histochemical analysis of *AHK4:GUS* lines upon mock inoculation (control) or infection with *R. fascians* D188. Expression patterns were visualized at 4 or 14 days post inoculation.
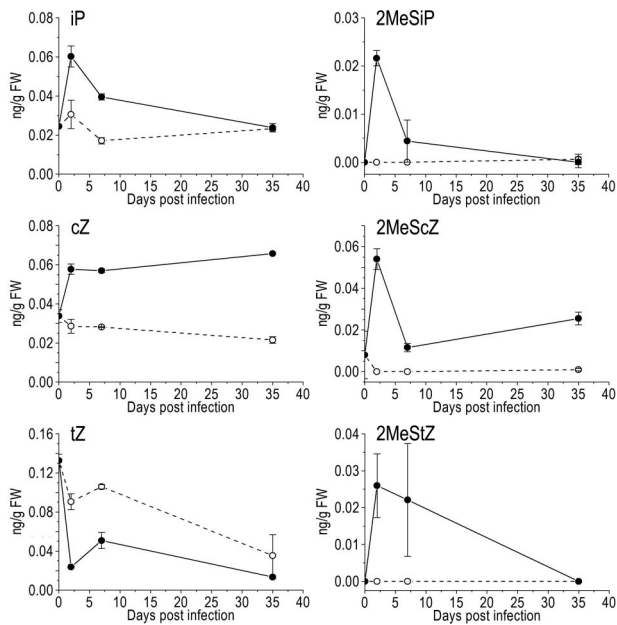
Fig. 4. Cytokinin profiles in *Arabidopsis* Col-0 shoots at different time points during the interaction with *R. fascians*. The respective CK base is indicated above each graph; mock-inoculated with water (dashed line, open circle), upon infection with strain D188 (full line, filled circle). Error bars represent SDs (*n* = 3).

the 6 *R. fascians* CK bases as substrates and ferricyanide (dehydrogenase activity) or oxygen (oxidase activity) as electron acceptors, at the physiological pH 6.0. The capacity of each CKX enzyme to degrade the CK bases was expressed as values relative to their ability to degrade iP (Table 1; for absolute enzymatic activities, see Table S1). Despite variations in substrate specificities, cZ and 2MeScZ were the worst substrates for all 3 apoplastic CKXs, which probably accounts for their accumulation in infected plants. Similar specificity patterns were observed for the CK ribosides (data not shown).

The *R. fascians* CKs Act Synergistically. The unusually strong outcome of infection with *R. fascians*, as compared with the relatively low CK levels detected in supernatants and infected plant tissues, might be caused partly by a synergistic action of the CK mix. Hence, the biological activity of the 6 identified CK bases was tested as individual molecules and as equimolar mixes in different bioassays relevant for the induced symptoms.

First, we assayed the response of *AHK4:GUS* reporter lines to the *R. fascians* CKs. Plants were transferred (at developmental stage 1.05; see *Materials and Methods*) to medium containing 10 µM of the individual CKs or CK mixes and analyzed histochemically after

10 days; iP, cZ, and tZ strongly activated the *AHK4* expression, whereas their 2MeS-derivatives had a more moderate effect (Fig. 5*A*). However, when plants were treated with an equimolar mix of iP, cZ, tZ, and their 2MeS-counterparts (eq6), activation levels equaled that obtained upon *R. fascians* infection (Figs. 2 and 5*A*).

Two other typical features of infected *Arabidopsis* plants are bleached leaves and anthocyanin accumulation (9). The contribution of the bacterial CKs to these phenotypes was determined by spectrophotometrical quantification of the chlorophyll, and the anthocyanin content in the aerial parts of plants grown for 10 days on medium containing 10 µM CKs. Treatment with the individual CKs caused bleaching and anthocyanin accumulation to different degrees (Fig. 5*B*). Interestingly, when compared with the calculated additive effect of the individual CKs (add4 and add6), a synergistic effect was observed for eq4 (iP, cZ, and their 2MeS-derivatives), but especially for eq6 (Fig. 5*B*).

The formation of shoots is the most characteristic phenotype induced on all host plants upon *R. fascians* infection. To evaluate the shoot induction capacity of the bacterial CKs, rooting, green callus development, and shoot formation were scored at 28 days post incubation in a callus and shoot regeneration assay starting from *Arabidopsis* root explants (see *Materials and Methods*); 2MeScZ and cZ displayed the lowest activity in this assay, but, again, a synergistic effect was observed for eq4 at 10 µM (Fig. 5*C*) and for eq6 at 1 µM (Fig. 5*D*; Fig. S4), when compared with the calculated add4 and add6.

This synergistic action was confirmed in a typical CK bioassay: deetiolation of dark-grown *Arabidopsis* seedlings. After 4 weeks of dark treatment, the deetiolation effect was quantified by scoring cotyledon opening and leaf formation; the hypocotyl length was not considered due to high variability. In this assay, the 2MeS-CK activities were lower than those of their classical counterparts. However, the number of leaf formation events was significantly higher for eq6 at 10 µM (data not shown) and 1 µM than the calculated add6 (Fig. 5*E*).

Last, *in planta* tissue proliferation is an essential aspect of the symptomatology (17). Therefore, the cell proliferative capacity of the 6 *R. fascians* CKs was quantified on CK-dependent tobacco callus by measuring the increase in fresh weight. The 2MeS-CKs had a significant proliferative potential, comparable with that of classical CKs at 10 µM (Fig. 5*F*). Interestingly, although at 100 µM, the classical CKs had a toxic effect, all 3 2MeS-derivates continued to stimulate cell proliferation.

Discussion

Previous data did not allow to unequivocally conclude whether bacterial CKs were involved in *R. fascians*-induced symptoms (7, 9, 13–18). Here, we addressed this question by evaluating the response of *Arabidopsis* on *R. fascians* infection at the level of CK perception. *Arabidopsis* has 3 CK receptors, AHK2, AHK3, and AHK4, with partly redundant but also divergent functions (24, 31), and an AHK-receptor-independent pathway as evidenced by the intact,

Table 1. Substrate specificity of apoplastic CKX enzymes of *Arabidopsis* in dehydrogenase (ferricyanide, FC) and oxygen (O₂) mode at pH 6.0 given as relative activities

Substrate	CKX2		CKX4		CKX6	
	FC	O_2	FC	O_2	FC	O_2
iP	100	100	100	100	100	100
2MeSiP	29	19	48	52	54	21
cZ	9	—	24	—	35	—
2MeScZ	2	—	9	—	17	—
tZ	30	111	83	97	30	56
2MeStZ	52	15	17	38	42	69

All data represent mean values of at least 2 biological replicates. Deviations between replicates did not exceed 10%; dashes, oxidative degradation of *cis*-derivatives could not be determined (see *Materials and Methods*).
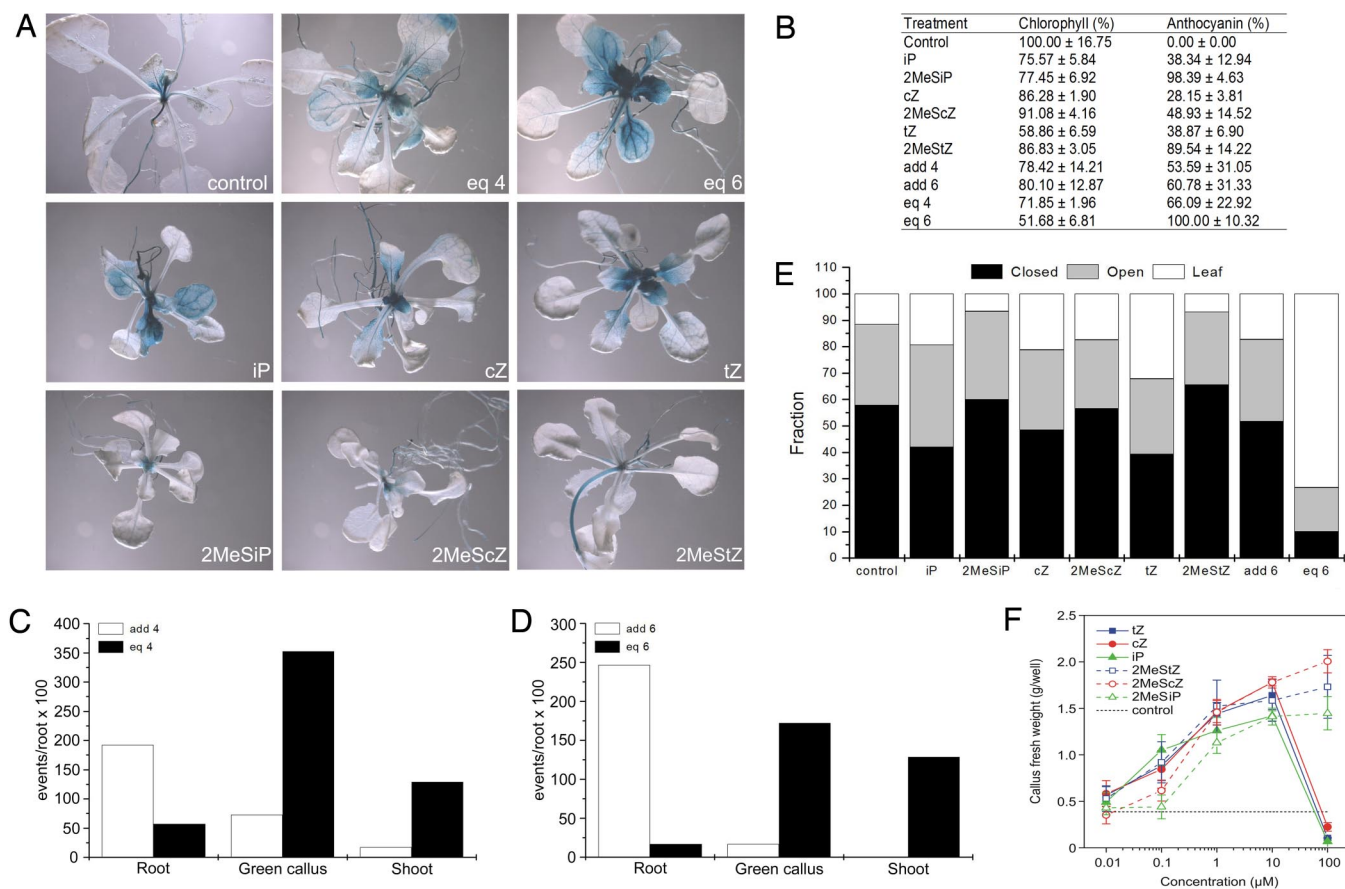
Fig. 5. Bioassays demonstrating the synergistic action of the *R. fascians* CK bases. Equimolar mixes or calculated additive effect of iP, 2MeSiP, cZ, and 2MeScZ (eq4, add4), and of iP, 2MeSiP, cZ, 2MeScZ, tZ, and 2MeStZ (eq6, add6). (*A*) Histochemical staining of the *AHK4:GUS* reporter line treated with 10 μM of the individual CKs or of the equimolar mixes for 10 days. (*B*) Loss of chlorophyll content and anthocyanin accumulation upon CK treatment. The chlorophyll content and anthocyanin accumulation are represented relative to untreated (control) plants and to eq6 treatment, respectively. Individual CKs, 10 μM; add4, average number of events provoked by the 4 CKs at 1 μM as a measure for the additive effect of these CKs; eq4, number of events provoked by the equimolar mix at a final concentration of 10 μM (containing 2.5 μM of each CK); add6 represents the average number of events provoked by the 6 CKs at 0.1 μM as a measure for the additive effect of these CKs; eq6, number of events provoked by the equimolar mix at a final concentration of 1 μM (containing 0.167 μM of each CK). (*C*) Root inhibition, and callus and shoot induction events observed in the regeneration assays; add4, average number of events provoked by the 4 CKs at 1 μM as a measure for the additive effect of these CKs; eq4, number of events provoked by the equimolar mix at a final concentration of 10 μM (containing 2.5 μM of each CK). (*D*) Root inhibition, and callus and shoot induction events observed in the regeneration assays; add6 represents the average number of events provoked by the 6 CKs at 0.1 μM as a measure for the additive effect of these CKs; eq6, number of events provoked by the equimolar mix at a final concentration of 1 μM (containing 0.167 μM of each CK). (*E*) Deetiolation of *Arabidopsis* plants on CK treatment. The number of events (closed or open cotyledons, and leaf formation) is given as percentages of the total number of germinated seedlings. Individual CKs, number of events scored at 1 μM; add6, sum of events scored for the 6 CKs at 1 μM; eq6, number of events scored for the equimolar mix at a final concentration of 6 μM (containing 1 μM of each CK). (*F*) Dose–response curve of the CK-dependent tobacco callus growth. The growth of untreated (control) callus is represented by the dotted line. Error bars represent SDs ($n = 6$).

although reduced, plant body formation of an *ahk2ahk3ahk4* mutant (31). Functional analysis demonstrated that either AHK3 or AHK4 are sufficient for symptom development, suggesting that both receptors are used in parallel for the recognition of the *R. fascians* CKs. Also, the nonresponsiveness of the *ahk3ahk4* mutant proved the crucial role of the bacterial CKs in the pathology. The AHK3 receptor is constitutively expressed in the shoot (24), has the broadest ligand perception range (26), and its expression is not significantly modified by the bacteria. *AHK4* is thought to be part of a specific recognition system (26), its expression is mainly located in the root (24), and upon infection it is ectopically expressed in the shoot. Altogether, these data suggest that AHK3 is probably the initial receptor for the *R. fascians* signals and that AHK4 increases the sensitivity of the aerial plant parts for the bacterial morphogens. AHK2, highly active in shoot tissue (24), and the putative AHK-receptor-independent pathway are seemingly not involved in recognition of the bacterial signals. The *ahk3ahk4* double mutant was much less responsive to exogenous CK treatment than the other 2 double mutants (Fig. S5), indicating that AHK2 has a lower

sensitivity or controls a more narrow downstream signaling cascade, possibly the reason that this receptor is not crucial in the *R. fascians* pathology.

Already since 1966, researchers have wondered which bacterial CKs were responsible for the *R. fascians*-induced phenotype (8, 10). Bacterial isolates had always been grown in relatively rich media, but from recent insights, we know that essential virulence genes are not expressed under these conditions (22, 27, 32). Therefore, we determined the CK profiles of strain D188 and its plasmid-free derivative D188–5 as reference, grown in defined minimal medium optimized for virulence gene expression (22). Six CK bases were detected: iP, 2MeSiP, cZ, 2MeScZ and, to a lesser extent, tZ and 2MeStZ. Riboside levels were 10-fold lower, but followed the same trends as the free bases (data not shown). Given their low overall concentration and their lower biological activity (26), the ribosides probably do not affect the pathology. Besides 2MeStZ, all of these CKs had been detected in supernatants of different *R. fascians* isolates (10–14), but the use of near-isogenic strains differing only in the occurrence of the linear plasmid allows a much stronger

Pertry *et al.*

correlation between these CKs and symptom development. Both strains produced the same CK spectrum, possibly explaining the problematic attribution of specific CKs to virulent strains (13, 14), but the presence of the linear plasmid strongly contributes to the secreted levels of iP, cZ, and 2MeScZ. Currently, the consensus is that cZ mainly (33) and 2MeS-derivates only (13, 34) originate from tRNA degradation. Because tRNA turnover rates are too slow (35) to account for the increased levels of iP, cZ, and 2MeScZ, we propose that these CKs are synthesized de novo by a linear plasmid-encoded machinery. The sequence of the linear plasmid of strain D188 did not reveal any CK biosynthetic genes besides the *fas* operon (I. Francis, unpublished results); therefore, this is the only plausible locus to encode the CK biosynthetic pathway (15, 22). The essential role of this pathway in the unique leafy gall pathology is further supported by the presence of a *fas*-like operon in the genome of the only other known leafy gall-inducing bacterium, *S. turgidiscabies* (21). Unexpectedly, no significant differences were detected when bacteria were grown under noninducing or inducing conditions for virulence gene expression. Presumably, laboratory media do not mimic the physiological conditions of plants, especially when intimate plant-pathogen interactions are considered (36). If so, the measured CK levels produced in vitro by *R. fascians* would be an underestimation of the true biosynthetic potential of the bacteria *in planta*.

The accumulation of cZ and 2MeScZ in infected tissues and the transient peak in the levels of iP, 2MeSiP, and 2MeStZ at the early interaction phase hinted at the biological significance of the identified bacterial CKs. The discrepancy with earlier reports in which the CK levels did not differ or even decreased upon infection (9, 17) might be entirely attributed to our extended CK profiling that included the 2MeS-CKs. To understand the differential kinetics of the CK levels in infected tissues, we determined the substrate specificities of apoplastic CKX enzymes that function in CK homeostasis. These enzymes did not efficiently degrade 2MeS-type CKs and *cis*-derivatives, probably affecting the accumulation of cZ and 2MeScZ in infected *Arabidopsis* tissues. Interestingly, the vacuolar CKX enzymes and CKX5 (30) displayed a very different substrate specificity and degraded the 2MeS- and, to some extent, the *cis*-derivatives more efficiently (Table S2). Possibly, these enzymes are involved in the removal of tRNA breakdown products during plant development. Intriguingly, when the CK profile of tobacco leafy galls was determined, cZ and 2MeScZ did not accumulate, but iP was built up instead (Fig. S6), as reported in *R. fascians*-infected pea plants (14). These observations suggest that the accumulation of specific bacterial CKs depends on the host, reflecting different substrate specificities of the plant homeostasis mechanisms. Consequently, by producing a spectrum of CKs, *R. fascians* might ensure that a subset of its morphogens is stable enough *in planta* to trigger plant developmental alterations, a strategy that might well be at the basis of its very broad host range.

Within the *R. fascians*-produced CKs, the biological activities of iP and tZ are generally recognized, whereas a true hormonal function has been reported for cZ only in a few plant species or organs (26, 37). To date, no morphogenic activity had been attributed to 2MeS-type CKs (25). We show that the complete set of bacterial CKs are recognized by the CK receptors AHK3 and AHK4 and have significant biological activities in 5 different bioassays, although the effect of the 2MeS-CKs was generally lower than that of their classical counterparts. More importantly, synergistic effects were observed when plants were treated with equimolar mixes of the bacterial CKs. In contrast to the classical CKs, the 2MeS-CKs had no cytotoxic effect within the tested concentration range in a tobacco callus bioassay. The continuous presence of the bacteria has been shown to be essential for symptom maintenance (38), and a constant delivery of morphogens into the apoplast might require less active and less toxic 2MeS-derivatives.

Based on the data presented, we propose the following model for the modus operandi of the *R. fascians* CKs in *Arabidopsis*. Initially,

the bacterial CKs are perceived by AHK3 and, in parallel, strongly activate *AHK4* expression in shoots, increasing the plant tissue sensitivity. The synergistic action of the CK mix leads to an upscaled response, initiating the developmental alterations. Feedback and homeostatic mechanisms activated in the plant result in the degradation of a subset of the bacterial CKs. However, the *Arabidopsis* CKX machinery is inadequate to eliminate all CKs of the bacterial mix and, consequently, cZ and the less toxic 2MeScZ accumulate in infected tissues. Therefore, these CKs are responsible for the continuous tissue proliferation and symptom maintenance. In conclusion, our data have uncovered the enigma of the *R. fascians* pathology: the persistent challenge with a complex mixture of synergistic CKs transforms nearly all plants into shooty niches. Although other plant pathogens might use a similar strategy to manipulate their hosts to their own advantage, to our knowledge, the "trick-with-the-CK-mix" is a novel concept in phytopathology.

Materials and Methods

Bacterial Strains and Growth Conditions. The *R. fascians* strains used were the pathogenic D188 that carries the linear virulence plasmid pFiD188 and its non-pathogenic plasmid-free derivative D188–5 (39). These strains were grown in liquid yeast extract broth at 28 °C for 2 days under gentle agitation until late exponential phase. For the determination of CKs in bacterial supernatants, 300-mL cultures were grown under control and optimized conditions for virulence gene expression as described previously (22).

Plant Material and Growth Conditions. *A. thaliana* seeds were sterilized and germinated as described (9). The *Arabidopsis* wild-type ecotype Columbia (Col-0) was obtained from the European *Arabidopsis* Stock Centre.

Infection, Chemical Treatment, and Sampling. Infections and treatments were repeated independently 3 times on 50 plants at the developmental stage 1.05 (16 days old with 5 visible leaves) (40). Plants were infected as described (9) and observed daily until 24 dpi for responsiveness scoring. For CK analyses, the aerial plant parts were sampled by snap freezing in liquid nitrogen at 0, 2, 7, and 35 dpi. For chemical treatment, the CKs (OlChemIm Ltd.) were dissolved in DMSO (Sigma-Aldrich) and added to Murashige and Skoog (MS) medium at concentrations ranging from 0.1 to 100 μM. Plants were transferred to the medium for 10 days and sampled for further analyses (phenotypic responsiveness, biological activity, and *GUS* expression).

Histochemical Staining. For GUS staining, the entire plant was sampled at 4 and 14 dpi or after 10 days of CK treatment, and subsequently stained and analyzed as described (9). The 3 biological repeats each consisted of at least 5 plants per treatment.

Bacterial and Plant CK Measurements. For measurement of classical CK levels, CKs were isolated, purified, and analyzed as described (41), with some modifications; 2MeS-CKs were quantified by LC-MS in multiple reaction-monitoring mode. For CK profiling of bacterial supernatants, 150 mL of cell-free cultures were extracted and used for 3 technical replicates; these analyses were independently repeated 3 times. For the plant CKs, 1 g of plant material was used in 3 biological repeats. The occurrence of 25 CK metabolites was evaluated, including isoprenoid and aromatic bases, their ribosides, and O- and N-glucosides.

E. coli Receptor Recognition Assay. *E. coli* KMI001 strains harboring plasmids pIN-III-AHK4 and pSTV28-AHK3 (42, 43) were used and assayed as described (26).

CKX Enzyme Assay. A detailed description of this procedure is given in *SI Methods* and Table S3.

Chlorophyll and Anthocyanin Measurements. Aerial plant parts were collected 10 days after CK treatment, ground in liquid nitrogen, and 100 mg of material was used per analysis. Chlorophyll was extracted and measured as described (44). Anthocyanins were quantified as described (45), with some modifications. In short, total pigments were extracted for 10 min in 0.75 mL of 1% HCl/methanol, and 0.5 mL of distilled H_2O was added. Chlorophyll was removed by chloroform extraction and the quantity of anthocyanin pigments in the aqueous/methanol phase was determined by measuring the absorbance at 530 nm minus that at 657 nm. All values were normalized to the fresh weight of each sample in 3 independent biological repeats.

Shoot Induction Assay. The *Arabidopsis* plants were grown for 8 days on MS medium. The roots were harvested, cut in 1-cm explants, placed on 2.2-μM 2,4-D for 6 days, and thereafter, on MS medium containing 0.9 μM indole-3-acetic acid (IAA) and different concentrations of individual CKs or CK mixes (ranging from 0.1 to 100 μM final concentration). As positive control, roots were placed on MS medium containing 0.9 μM IAA and 5 μM iP, and on 0.9 μM IAA as negative control. Phenotypes (root, callus, or shoot formation) were scored at 28 dpi and represented as (events/root) $\times$ 100. When the entire root explant developed into callus or shoot, an arbitrary score of 10 was assigned. At least 20 root explants were used per treatment.

Deetiolation Assay. We placed 10 *Arabidopsis* seeds for 24 h in continuous light on MS medium containing 1 or 10 μM of the individual CKs or a mix of 1 or 10 μM of each of the 6 *R. fascians* CKs, and then transferred them to the dark. However, in the presence of relatively high amounts of CKs, the hypocotyl length is strongly reduced, the apical hook is lost, cotyledons open, and green leaves are formed (46). After 4 weeks, cotyledon opening and leaf formation were scored. The assay was repeated 3 times and the observed phenotypes are given as the percentage of events on the total number of germinated seedlings in the 3 experiments.

Tobacco Callus Bioassay. The stimulation of CK-dependent growth of tobacco (*Nicotiana tabacum* L. cv. Wisconsin 38) callus was measured as described (47), with minor modifications. The callus was grown in 6-well plates (3 mL of MS medium per well). The final concentration of DMSO in the media did not exceed 0.2%. Six replicates were prepared for each CK concentration and the experiments were repeated at least twice.

1. Tsavkelova EA, Klimova SY, Cherdyntseva TA, Netrusov AI (2006) Microbial producers of plant growth stimulators and their practical use: A review. *Appl Biochem Microbiol* 42:117–126.
2. Robert-Seilaniantz A, Navarro L, Bari R, Jones JDG (2007) Pathological hormone imbalances. *Curr Opin Plant Biol* 10:372–379.
3. Barash I, Manulis-Sasson S (2007) Virulence mechanisms and host specificity of gall-forming *Pantoea agglomerans*. *Trends Microbiol* 15:538–545.
4. Sisto A, Cipriani MG, Morea M (2004) Knot formation caused by *Pseudomonas syringae* subsp. *savastanoi* on olive plants is *hrp*-dependent. *Phytopathology* 94:484–489.
5. Zhu J, et al. (2000) The bases of crown gall tumorigenesis. *J Bacteriol* 182:3885–3895.
6. Vereecke D, Cornelis K, Temmerman W, Holsters M, Goethals K (2002) Versatile persistence pathways for pathogens of animals and plants. *Trends Microbiol* 10:485–488.
7. Goethals K, Vereecke D, Jaziri M, Van Montagu M, Holsters M (2001) Leafy gall formation by *Rhodococcus fascians*. *Annu Rev Phytopathol* 39:27–52.
8. Thimann KV, Sachs T (1966) The role of cytokinins in the "fasciation" disease caused by *Corynebacterium fascians*. *Am J Bot* 53:731–739.
9. Depuydt S, et al. (2008) Modulation of the hormone setting by *Rhodococcus fascians* results in ectopic *KNOX* activation in Arabidopsis. *Plant Physiol* 146:1267–1281.
10. Helgeson JP, Leonard NJ (1966) Cytokinins: Identification of compounds isolated from *Corynebacterium fascians*. *Proc Natl Acad Sci USA* 56:60–63.
11. Scarbrough E, Armstrong DJ, Skoog F, Frihart CR, Leonard NJ (1973) Isolation of *cis*-zeatin from *Corynebacterium fascians* cultures. *Proc Natl Acad Sci USA* 70:3825–3829.
12. Armstrong DJ, Scarbrough E, Skoog F, Cole DL, Leonard NJ (1976) Cytokinins in *Corynebacterium fascians* cultures. Isolation and identification of 6-(4-hydroxy-3-methyl-*cis*-2-butenylamino)-2-methylthiopurine. *Plant Physiol* 58:749–752.
13. Murai N, Skoog F, Doyle ME, Hanson RS (1980) Relationships between cytokinin production, presence of plasmids, and fasciation caused by strains of *Corynebacterium fascians*. *Proc Natl Acad Sci USA* 77:619–623.
14. Eason JR, Morris RO, Jameson PE (1996) The relationship between virulence and cytokinin production by *Rhodococcus fascians* (Tilford 1936) Goodfellow 1984. *Plant Pathol* 45:323–331.
15. Crespi M, Messens E, Caplan AB, Van Montagu M, Desomer J (1992) Fasciation induction by the phytopathogen *Rhodococcus fascians* depends upon a linear plasmid encoding a cytokinin synthase gene. *EMBO J* 11:795–804.
16. Balázs E, Sziráki I (1974) Altered levels of indoleacetic acid and cytokinin in geranium stems infected with *Corynebacterium fascians*. *Acta Phytopathol Acad Sci Hung* 9:287–292.
17. de O Manes C-L, Van Montagu M, Prinsen E, Goethals K, Holsters M (2001) De novo cortical cell division triggered by the phytopathogen *Rhodococcus fascians* in tobacco. *Mol Plant-Microbe Interact* 14:189–195.
18. Galis I, Bilyeu K, Wood G, Jameson PE (2005) *Rhodococcus fascians*: Shoot proliferation without elevated cytokinins. *Plant Growth Regul* 46:109–115.
19. Akiyoshi DE, Regier DA, Gordon MP (1987) Cytokinin production by *Agrobacterium* and *Pseudomonas* spp. *J Bacteriol* 169:4242–4248.
20. Stange RR, et al. (1996) PCR amplification of the *fas-1* gene for detection of virulent strains of *Rhodococcus fascians*. *Plant Pathol* 45:407–417.
21. Joshi MV, Loria R (2007) *Streptomyces turgidiscabies* possesses a functional cytokinin biosynthetic pathway and produces leafy galls. *Mol Plant-Microbe Interact* 20:751–758.
22. Temmerman W, et al. (2000) Leafy gall formation is controlled by *fasR*, an AraC-type regulatory gene, in *Rhodococcus fascians*. *J Bacteriol* 182:5832–5840.
23. Inoue T, et al. (2001) Identification of CRE1 as a cytokinin receptor from *Arabidopsis*. *Nature* 409:1060–1063.
24. Higuchi M, et al. (2004) *In planta* functions of the *Arabidopsis* cytokinin receptor family. *Proc Natl Acad Sci USA* 101:8821–8826.
25. Matsubara S (1980) Structure-activity relationships of cytokinins. *Phytochemistry* 19:2239–2253.
26. Spíchal L, et al. (2004) Two cytokinin receptors of *Arabidopsis thaliana*, CRE1/AHK4 and AHK3, differ in their ligand specificity in a bacterial assay. *Plant Cell Physiol* 45:1299–1305.
27. Cornelis K, Maes T, Jaziri M, Holsters M, Goethals K (2002) Virulence genes of the phytopathogen *Rhodococcus fascians* show specific spatial and temporal expression patterns during plant infection. *Mol Plant-Microbe Interact* 15:398–403.
28. de O Manes CL, et al. (2004) Phenotypic alterations in *Arabidopsis thaliana* plants caused by *Rhodococcus fascians* infection. *J Plant Res* 117:139–145.
29. Cornelis K, et al. (2001) The plant pathogen *Rhodococcus fascians* colonizes the exterior and interior of the aerial parts of plants. *Mol Plant-Microbe Interact* 14:599–608.
30. Werner T, et al. (2003) Cytokinin-deficient transgenic Arabidopsis plants show multiple developmental alterations indicating opposite functions of cytokinins in the regulation of shoot and root meristem activity. *Plant Cell* 15:2532–2550.
31. Riefler M, Novak O, Strnad M, Schmülling T (2006) *Arabidopsis* cytokinin receptor mutants reveal functions in shoot growth, leaf senescence, seed size, germination, root development, and cytokinin metabolism. *Plant Cell* 18:40–54.
32. Maes T, et al. (2001) The *att* locus of *Rhodococcus fascians* strain D188 is essential for full virulence on tobacco through the production of an autoregulatory compound. *Mol Microbiol* 42:13–28.
33. Miyawaki K, et al. (2006) Roles of *Arabidopsis* ATP/ADP isopentenyltransferases and tRNA isopentenyltransferases in cytokinin biosynthesis. *Proc Natl Acad Sci USA* 103:16598–16603.
34. Prinsen E, Kamínek M, Van Onckelen HA (1997) Cytokinin biosynthesis: A black box? *Plant Growth Regul* 23:3–15.
35. Klämbt D, Holtz J, Helbach M, Maass H (1984) Die Biogenese der Cytokinine. *Ber Dtsch Bot Ges* 97:57–65.
36. Marco ML, Legac J, Lindow SE (2005) *Pseudomonas syringae* genes induced during colonization of leaf surfaces. *Environ Microbiol* 7:1379–1391.
37. Yonekura-Sakakibara K, Kojima M, Yamaya T, Sakakibara H (2004) Molecular characterization of cytokinin-responsive histidine kinases in maize. Differential ligand preferences and response to cis-zeatin. *Plant Physiol* 134:1654–1661.
38. Vereecke D, et al. (2000) The *Rhodococcus fascians*-plant interaction: Morphological traits and biotechnological applications. *Planta* 210:241–251.
39. Desomer J, Dhaese P, Van Montagu M (1988) Conjugative transfer of cadmium resistance plasmids in *Rhodococcus fascians* strains. *J Bacteriol* 170:2401–2405.
40. Boyes DC, et al. (2001) Growth stage-based phenotypic analysis of Arabidopsis: A model for high throughput functional genomics in plants. *Plant Cell* 13:1499–1510.
41. Novák O, et al. (2003) Quantitative analysis of cytokinins in plants by liquid chromatography–single-quadrupole mass spectrometry. *Anal Chim Acta* 480:207–218.
42. Yamada H, et al. (2001) The Arabidopsis AHK4 histidine kinase is a cytokinin-binding receptor that transduces cytokinin signals across the membrane. *Plant Cell Physiol* 42:1017–1023.
43. Suzuki T, et al. (2001) The Arabidopsis sensor His-kinase, AHK4, can respond to cytokinins. *Plant Cell Physiol* 42:107–113.
44. Peng J, Harberd NP (1997) Gibberellin deficiency and response mutations suppress the stem elongation phenotype of phytochrome-deficient mutants of Arabidopsis. *Plant Physiol* 113:1051–1058.
45. Feinbaum RL, Ausubel FM (1988) Transcriptional regulation of the *Arabidopsis thaliana* chalcone synthase gene. *Mol Cell Biol* 8:1985–1992.
46. Chory J, Reinecke D, Sim S, Washburn T, Brenner M (1994) A role for cytokinins in de-etiolation in *Arabidopsis*. *det* mutants have an altered response to cytokinins. *Plant Physiol* 104:339–347.
47. Holub J, Hanuš J, Hanke DE, Strnad M (1998) Biological activity of cytokinins derived from *ortho*- and *meta*-hydroxybenzyladenine. *Plant Growth Regul* 26:109–115.